LES INVESTIGATION OF THE HYSTERESIS REGIME IN THE COLD MODEL OF A SWIRL BURNER

M. Hadžiabdić
International University of Sarajevo
Hrasnička cesta 15, 71000 Sarajevo,
Bosnia and Herzegovina
mhadziabdic@ius.edu.ba

R. Mullyadzhanov
Novosibirsk State University and
Institute of Thermophysics SB RAS
Pirogova St 2, 63090 Novosibirsk, Russia
rustammul@gmail.com

K. Hanjalić
Novosibirsk State University
Pirogova St 2, 63090 Novosibirsk, Russia
khanjalic@gmail.com

ABSTRACT

We report on large-eddy simulation of flow in a cold replica of a non-premixed swirl burner in which hysteresis was detected when transiting from an attached long flame to a short lifted flame and vice versa (Hübner et al. 2003, Tummers et al. 2008). The unconfined highly swirling annular jet is generated by rotating the outer pipe of the annular air supply at 4000 rpm, while gas is fed through an inner annulus. The swirl number, controlled by the flow rate, range from 2.8 for the stable ("blue" flame) to 4.9 for the unstable ("yellow" flame). The air and fuel Reynolds numbers are 11250 and 2250 respectively for the maximum, to 6400 and 1300 for the minimum flow rate case. The LES results agree well with the available experimental data, reproducing notably different sizes and strengths of the central recirculation bubbles in the stable and unstable jets. It is shown that the flow undergoes different adjustments when approaching from different initial states to a state in the hysteresis region where both, the stable and unstable combustion regimes have been observed experimentally at the same swirl number of 3.26.

INTRODUCTION

Swirling motion imposed on flames is widely applied for stabilizing industrial burners. A low-pressure region in the jet core, created by a sufficiently strong swirl, causes a breakdown of the elongated attached but unstable vortex and formation of a short, lifted, stable toroidal structure. The separation bubble created or enhances by the swirl motion enhances recirculation of the combustion products thus providing a continuous and stable source of heat for flame ignition. The enhanced shear in the enveloping curved shear-layer augments the mixing and combustion. However, the trend may be reversed for a high rotation at too low axial flow rates due to local suppression of mixing and momentum transfer, and lead even to local laminarization.

Swirling jets have attracted much attention among the research community not only because of their industrial relevance, but also because of a number of interesting physical phenomena. Destabilization and stabilization depending on the swirl strength and flow configuration, augmentation of turbulence generation, vortex breakdown at strong swirls, effects of confinement and pressure field, secondary shear and strain rates due to streamline curvature and rotation, are only some of the features that attract attention. But numerical predicting of jets with high swirl rates poses still much of a challenge.

The vortex breakdown plays a significant role in the transition from one flow pattern to another. A number of researchers have detected hysteresis, i.e. that transition from one to another regime can occur at different conditions, and also that different regimes can take place at the same conditions, all depending on whether the transition is approached from a stable lifted flame to the unstable attached flame or vice versa.

While experimental evidence on flame hysteresis is well documented, few computational results dealing with this phenomenon are available in the literature. Several recent LES of flows relevant to the configuration here considered reproduced the main flow features and turbulence statistics generally in accord with the available experimental data, e.g. Wang et al. (2004), Facciolo et al., (2007), Garcia et a. (2006), Jones at al. (2012), among others. However, most published numerical simulations (LES and DNS) of swirling jets are limited to low to moderate swirls and relatively low Reynolds number. Moreover, most studies focus just on one configuration and regime, but little has been reported on numerical investigation of transition from one to another regimes and the effect of the initial flame state on the flows in the hysteresis region. Also, most numerical studies consider confined swirling flows with no free entrainment, which are generally more stable and pose less uncertainty in defining and treating the inflow and open boundary conditions.

In an experiment with a rotary-pipe swirl burner Hübner et al, (2003) and Tummers et al. (2008) found that the flame changes from a long, sooty (yellow) flame to a much shorter, onion-shaped (blue) lifted flame as the flow rates are increased at a constant air-to-fuel ratio and a sufficiently high rotation rate (> 3500 rpm), Fig 1. The opposite happens when increasing flow rate of a yellow flame, but the transition to a stable blue flame occurred at a much higher flow rate for the same rotation.

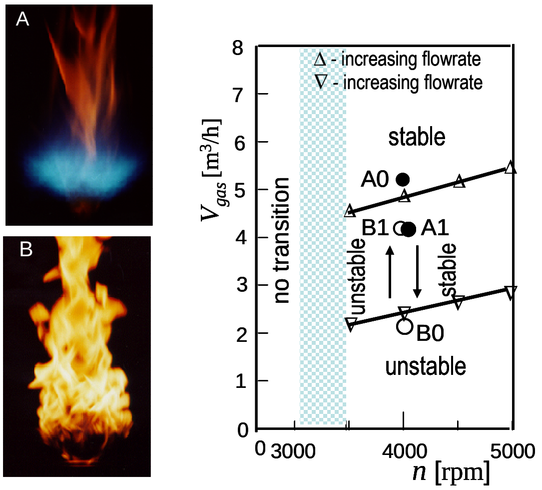

Fig. 1: Views of stable (A) and unstable (B) flames (left) and the stability diagram with hysteresis region. (Hübner et al.2003)

Moreover, in the intermediate range both regimes have been detected at the same conditions, depending from which side this state is approached. Because of the solid rod placed centrally in the burner, both flames contain recirculation bubbles. However, in contrast to a relatively weak recirculation in the yellow flame, the recirculation bubble in the blue flame is larger and stronger. While the upward transition occurs suddenly, the downward transition is characterized by gradual and unstable changes in the flame shape. As shown in Fig 1 right, the downward transition allows the blue flame in the range of the flow rates previously characterized by the yellow flame in the upward transition.

Hübner et al. (2003) detected a hysteresis also in cold flows in the same configurations, tough in a milder form compared to the flame where the effects of density variation in combusting situations may be significant.

We report on LES study of flow in a computational cold replica of the experiment of Hübner et al. focusing on the experimentally observed hysteresis. The aim is to gain an insight into and better understanding of the mechanism and conditions that lead to different flow regimes under the same controlling parameters. The high rotation number, defined as a ratio of maximal tangential velocity and the bulk axial velocity, $N = U_{\theta wal} / U_{bulk}$ is another novelty of the research. It ranges from 2.8 for the maximum flow rate case, to 4.9 for the minimal flow rate case. A role of vortex breakdown in formation of dominant flow pattern has also been investigated.

The large eddy simulations should make it possible to investigate the effects of the vortical and turbulence structure at very strong swirl and its effect on the transition from one to another regime. This work is a follow-up of an earlier RANS study (Hadžiabdić et al. 2012) and is also a precursor for the simulation of the reacting case which should mimic the full experiment.

We considered four cases corresponding to the experiment, indicated in Fig 1 rigt by A0, A1, B1 and B0. It is recalled that A0 corresponds to a fully stable (blue) flame at N=2.8, B0 to an unstable (yellow|) flame at N=4.9, whereas A1 and B1 correspond to a stable and unstable flame detected at the same conditions (N=3.16) when approaching from the stable and unstable flame respectively. The conditions for the four cases are summarised in Table 1, (velocities in m/s).

Case	N	U_{gas}	U_{air}	Re_{gas}	Re_{air}
A0	2.80	4.14	5.20	2250	11250
A1	3.26	3.30	4.16	1750	9700
B1	3.26	3.30	4.16	1750	9700
B0	4.91	2.38	3.00	1300	6400

Table 1: flow parameters of the cases considered

FLOWS AND COMPUATIONAL DETAILS

The flow considered is a cold model of the rotary-pipe swirl burner investigated experimentally by Hübner et al, (2003) and Tummers et al (2008). The burner is made of two 1320 mm long concentric annular ducts with the outer and inner diameters of 70.3 and 38 mm (air), and 32 and 24 mm (gas), respectively, and a solid rod of 24 mm dia placed at the centre. The swirl is generated in the outer (air) annulus by rotating its outer wall at a constant speed of 4000 rpm. The swirl number was imposed by adjusting the flow rate to replicate the experiment. The air and fuel Reynolds numbers (based on the hydraulic diameters) are ranged from 11250 and 2250 respectively, for the maximum to 6400 and 1300 for minimum flow rate case.

The LES was performed using the TU Delft unstructured finite-volume computational code T-FlowS. The filtered Navier-Stokes and continuity equations for incompressible fluid were closed by the dynamic Smagorinsky subgrid-scale model. The diffusion and convection terms in the momentum equations are discretised by the second-order central-difference scheme, whereas the time-marching was performed using a fully-implicit three-level time scheme. The computational domain shown consists of a cylinder of 12D diameter and 16D height (where D=70.3 mm denoting the rotating wall inner diameter is used throughout the paper as the characteristic dimension). The convective outflow is imposed at the exit boundary, while constant pressure was imposed on the open lateral boundary. A small co-flow with a velocity profile from RANS with a maximum of 5%U_b was imposed at the bottom free boundary at - 1.0D. It is reported by several authors that the influence of the co-flow boundary is minor as long as the co-flow is mild, (Hadziabdic & Hanjalic 2008, Garcia et al. 2007. No-slip condition was imposed for velocity at all wall boundaries.

In order to have the inflow condition as close as possible to the reference experiments, the two coaxial (non-swirling and swirling) annular jets entering the burner have been generated by precursor LES of flows in the preceding annular passages over the actual finite ducts length. The velocity field from these simulations was recorded and stored at every time step. These data were subsequently used to define the inflow velocity components for the two coaxial jets.

The mesh consists of about 13 mill hexahedral cells ($N_z \times N_r \times N_\theta$=210×228×264) clustered towards the burner mouth to resolve the steep gradients of the entry velocity. The maximum wall distance of the centre of the wall-adjacent cells expressed in wall units was less than 1. The mesh resolution quality was checked by comparing the characteristic mesh size $\Delta = [\Delta z \times \Delta r \times r\Delta\theta]^{1/3}$ with the Kolmogorov length scale $\eta = (\nu^3/\varepsilon)^{1/4}$ (with the dissipation rate ε taken from the RANS solution of the same flow, Hadžiabdić et al. (2012). The maximum Δ/η was everywhere less than 12, apart from the region very close to the burner mouth where it reached the value of 16, thus in accord with the common criterion for a sufficiently fine LES mesh quality.

The computations of cases A1 and B1 have been done by starting from the fully convergent solutions of their stable counterparts, A0 and B0, with a step-adjustment of the flow rate to the value corresponding to A1/B1cases.

RESULTS

Time averaged and instantaneous flow fields

Figure 2 provides an overview of the time-averaged recirculation bubbles for the two reference cases, the stable A0 and the unstable B0 configuration. In contrast to the combusting cases, the A0 bubble is smaller, enveloped by strong and symmetric axial motion (though a bit asymmetric), whereas the B0 bubble is much larger, asymmetric and unsettled with some streamlines wiggles above the stagnation point despite a long averaging period. However, the averaged negative velocity over the area from the centre to the “eye” of the bubble, is considerably higher in the A0 than in the B0 case (0.21 versus 0.09 of U_{bulk}), testifying of a substantially stronger recirculation, as could be expected in view of a much stronger shear in the shear layer encompassing the bubble.

The bubble size and shape for the A0 and A1 case agree well with the experimental data of Hübner (2010). The computed length of the recirculation zone 0.76*D* compared with the measured value 0.72*D*. The agreement with experiments is also confirmed by comparison of the measured and simulated mean velocity profiles (normalised with the bulk velocity $U_{0bulk,}$), shown in Fig 3. The axial and radial velocities agree very well with the measured data. A small discrepancy in the sharp peaks at r/R≈0.45 (outflow from the inner (“gas”) duct) immediately after the nozzle exit (z/D=0.11) is probably due to insufficient experimental resolution.

The experimental data for the tangential velocity in the cold regime are not available. Because of the same imposed hydrodynamics, we compare computations with the data obtained in the A0 flame. Indeed, the computed tangential velocity shows similar shapes as the measured ones at all axial locations, except that the experimental profiles are shifter towards the jet periphery as expected due to strong thermal expansion.

For comparison, LES results for the A1 case are also shown, but no experimental data for the cold regime are available. The visual images of the A0 and A1 flames look very similar, but because of a difference in the axial flow (about 20% in the bulk velocity) some modifications of the velocity field are expected. These are visible in all profiles hinting at the bubble widening and larger entrainment, as indicated by a larger radial velocity at z/D=0.28, and a faster decay in the axial and tangential velocity. A broader overview of the flow structure over the larger domain (up to z/D≈6) for all four cases is given in Fig 4 showing the tangential and axial velocity fields together with the streamlines. One can see that the A1 and B1 bubbles are similar in size (as expected in view of the same flow conditions), though but the B1 bubble is somewhat larger, more asymmetric and less settled.

The above observations are also reflected in the instantaneous field, illustrated in Fig. 5. While the A0 streamlines, despite wiggles, show unidirectional axial flow everywhere above the bubble, and a strong entrainment of the surrounding flow below it (smooth, close to hemispherical streamlines), the B0 picture shows some irregular recirculating patches within and above the bubble and much more nonuniform tangential velocity field. The A1 and B1 cases are relatively similar, though both showing some features of their stable counterparts.

Transients from stable to unstable regimes

The evolution of the jets approaching the intermediate states A1 and B1 when starting from A0 and B0 respectively, is illustrated in Fig 6 by selected snapshots of the instantaneous tangential and axial velocities and streamlines shown at the time instants (expressed in terms of the flow-through time $\tau = D/U_{bulk}$) after the start of the computations from the respective stable cases A0 and B0. While the transition from A0 (with relatively stable close-to-parallel streamline pattern) to A1 proceeds very fast exhibiting clearly destabilization effects already after τ=4 and reaching the well-established A1 case (with a somewhat larger recirculation bubble than in A0) after τ≈ 20, the B0 to B1 proceeds much more slowly and takes over a hundred of flow-through times to reach a typical, though still rather unstable B1 state. In both cases one sees a gradual change of the bubble size, with the end states A1 and B1 showing some similarity, but still being sufficiently different to confirm different stability sates despite the equal flow conditions. The B0 to B1 transition is especially interesting, as an increase in the axial velocity shows a clear trend to pull and elongate the initial bubble while contracting its radial dimension. A small dipole forms at the nozzle, grows displacing and eventually breaking up the original bubble into a smaller attached one and a secondary recirculation above it, which is swiftly convected along the flow, until eventually only the basic bubble sustains.

CONCLUSIONS

The LES simulations of isotherrnal model of a flame experiment reproduced the conditionally stable regimes (A0) well in accord with the available experimental data, thus providing credibility in the LES of other cases, the unstable B0 and the two cases at equal conditions, A1 and B1 supposed to correspond to the hysteresis region. Differences between the computed cold A1 and B1 have been detected, though substantially smaller than observed experimentally in flames. Due to the uncertainty in how weaker is the hysteresis in the cold flow, at this stage it is difficult to say if the simulations actually reproduced the phenomenon. Possibly, the transitions from one to another regime occurs also at different conditions in a cold flow than in flames, where a sudden flame lift-off can much easier be detected. The issue will hopefully be clarified after the computations are continued from the A0 to A1 transition further to B0, and the B0 to B1 further to A0, which are currently in progress.

REFERENCES

.Billant, P., Chomaz, J., Huerre, P. (1998). Experimental study of vortex breakdown in swirling jets. *J. Fluid Mech*. 376, 183–219.

Dunham, D., Spencer, A., McGuirk J.J., Dianat M (2009) Comparison of unsteady Reynolds-averaged Navier-Stokes and Large Eddy Simulation computational fluid dynamics methodologies for air swirl fuel injectors. *ASME: J Eng Gas Turb Power* 131:011,502–2

Facciolo, L., Tillmark, N., Talamelli, A., Alfredsson, P., (2007). A study of swirling turbulent pipe and jet flows. *Physics of Fluids* 19, 035105.

Garcia-Villalba, M., Fröhlich, J., Rodi, W. (2006). Identification and analysis of coherent structures in the near field of a turbulent unconfined annular swirling jet using large eddy simulation. *Physics of Fluids*, 18(5), 055103-055103-17.

Grinstein, F., Young, T, Gutmark EJ, Li G, Hsiao G, Mongia H (2002) Flow dynamics in a swirl combustor. *J. Turbulence* 3, 30–30(1)

Hadžiabdić, M. Halilagić, M., Hanjalić, K. (2012) RANS investigation of hysteresis of vortex breakdown in the cold models of a swirl burner, In K. Hanjalić et al (Eds) *Turbulence, Heta and Mass Tranfer 7*, Begell House Inc.

Hadžiabdić, M., Hanjalić, K. (2008) Vortical structures and heat transfer in a round impinging jet. *J. Fluid Mech*. 596, 221-260.

Hübner, A.W., (2010) PhD thesis (unfinished), Delft University of Technology, The Netherlands (M. Tummers, www.msp.tudelft.nl)

Hübner, A.W., Tummers, M., Hanjalic, K., Van der Meer, Th.H. (2003). Experiments on a swirl stabilized turbulent flame. *Experimental thermal and fluid science*. 27, 481–489.

Jochmann, P., Sinigersky, M., Hehle, M., Schäfer, O., Koch R., and Bauer, H.-J. (2006), Numerical simulation of processing vortex breakdown, *Int. J. Heat and Fluid Flow*, 27, 192-203.

Jones, W., Lentini, D. (2008). A realisable non-linear eddy viscosity/diffusivity model for confined swirling flows. *Int. J. Heat and Fluid Flow* 29, 1612–1627.

Jones, W.P., Lyra, S., Navarro-Martinez, S. (2012). Large eddy simulation of turbulent confined highly swirling annular flows, *Flow, Turbulence and Combustion*, Online publication, DOI: 10.1007/s10494-012-9402-3

Liang, H. Maxworthy, T. (2005). An experimental investigation of swirling jets. *J. Fluid Mech*. 525, 115–159.

Tummers, M., Hubner, A.W., Ven Veen, E., Hanjalic, K., Van der Meer Th.H. (2008). Hysteresis and transition in swirling nonpremixed flames. *Combustion and Flame* 156, 447–459.

Wang P, Bai X, Wessman M, Klingmann J (2004) Large eddy simulation and experimental studies of a confined turbulent swirling flow. *Phys Fluids* 16(9):3306–3324.

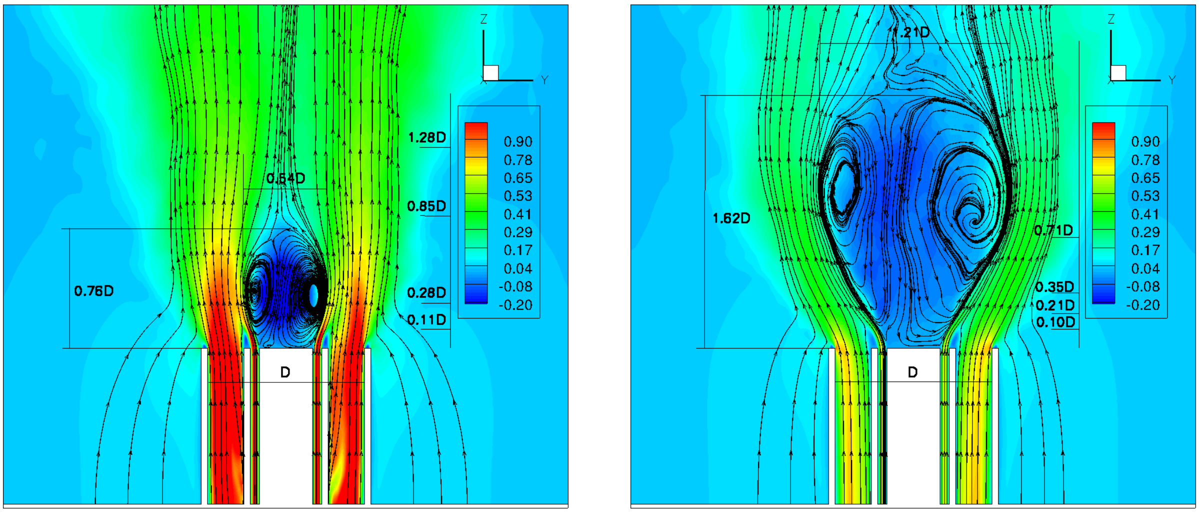

Fig . 2 A close look at the burner near-field axial velocity field . Left: A0, N=2.8; right: B0, N=4.91

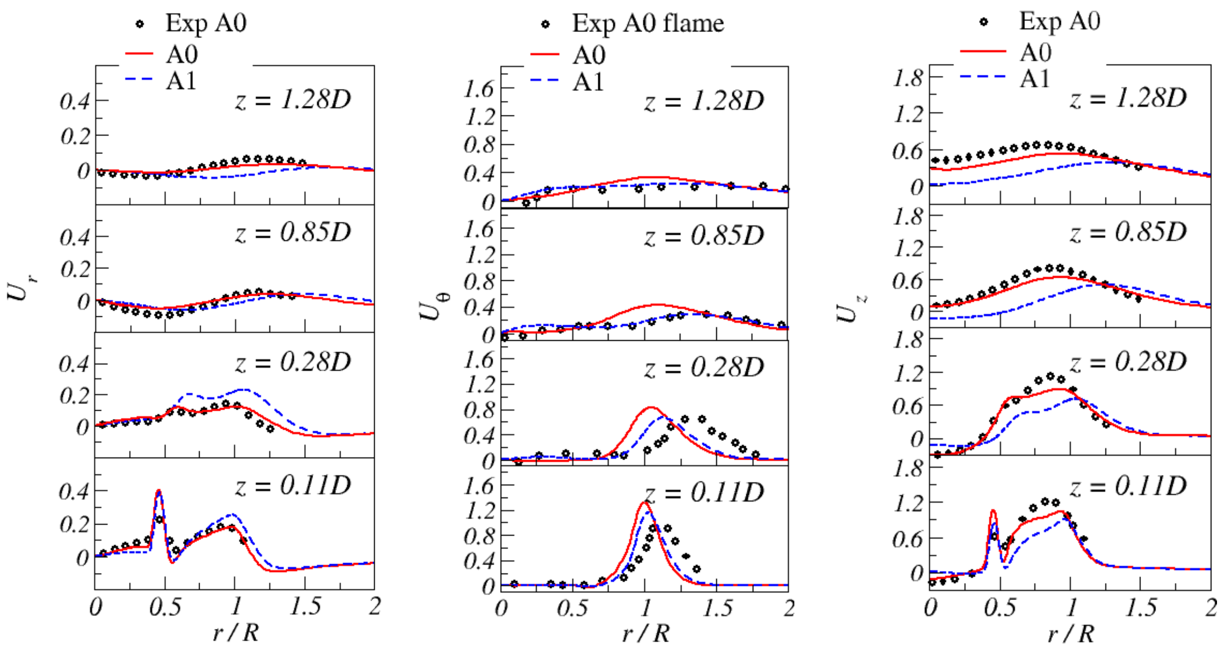

Fig. 3 Comparison of velocity profiles for A0 and A1 cases. From left to right: radial, tangential and axial components. Symbols: experiments for the A0 case. Note: axial and radial velocities are for the cold A0 and the tangential velocity for the A0 flame.

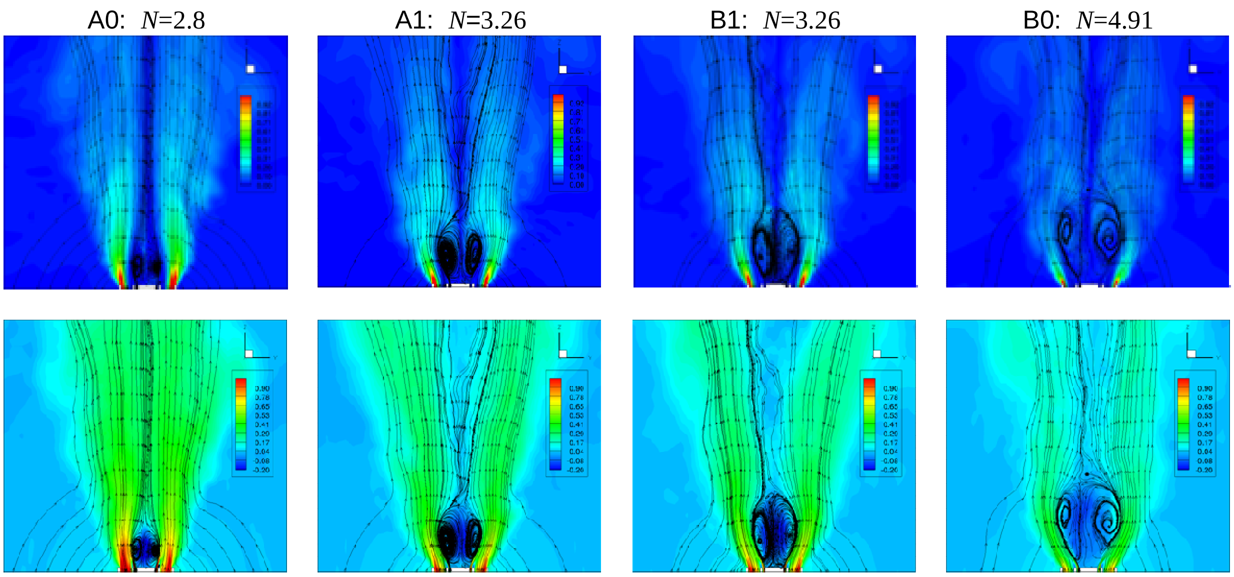

Fig. 4 Comparison of mean velocity components and streamlines in the vertical cut plane for the four cases considered. Top: tangential velocity, bottom: axial velocity.

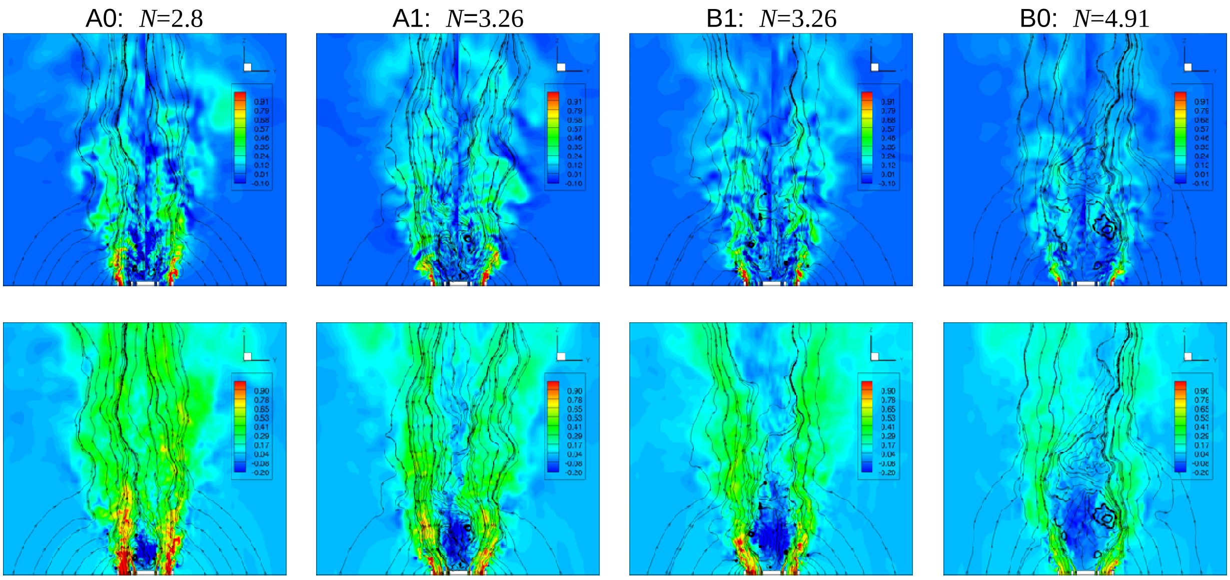

Fig. 5 Snapshots of instantaneous velocity fields in different regimes. Top: tangential velocity; bottom: axial velocity

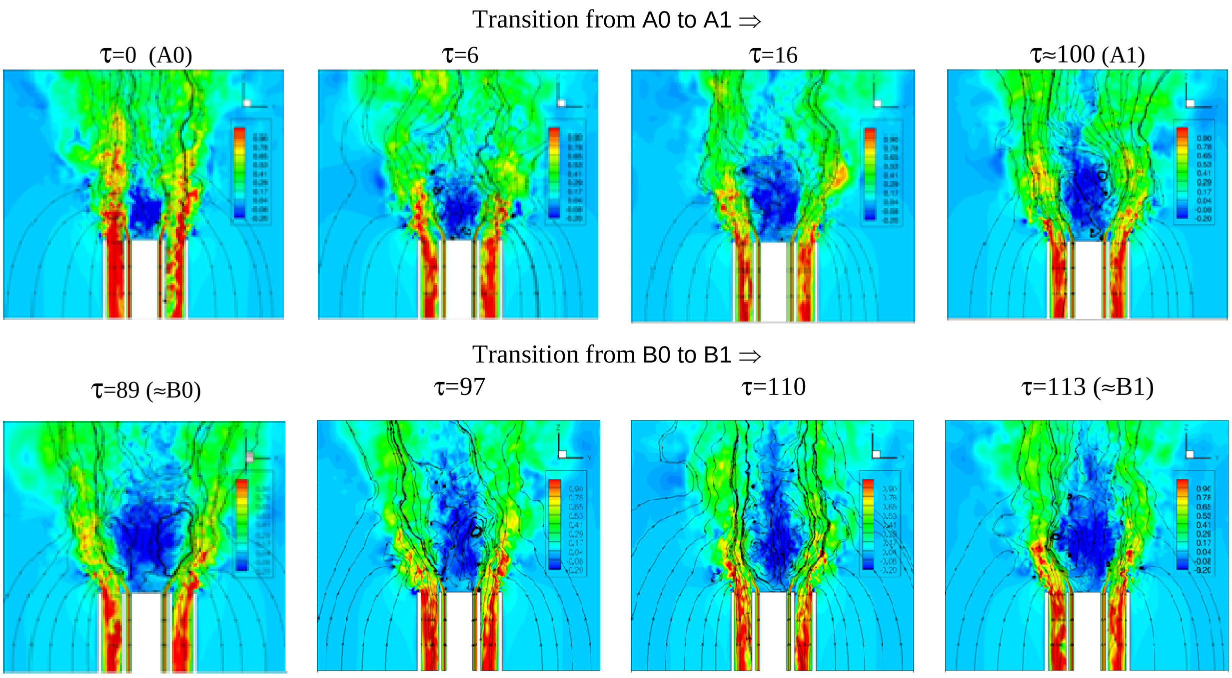

Fig. 6 Time evolution of the instantaneous streamline patterns and axial velocity field in the development of the B1 regime when starting from B0 (top) and of the A1 regime when starting from A0.